

Effect of Heat Treatment on Chip Formation in a Case Hardening Steel

Kumar Babu Surreddi^{*1}, Karin Björkeborn^{1,2}, Uta Klement¹

¹Department of Materials and Manufacturing Technology, Chalmers University of Technology, 412 96 Gothenburg, Sweden

²Scana industrier ASA, Norway

^{*1}surreddi@chalmers.se; ²kb@scana.se; ³uta.klement@chalmers.se

Abstract- In manufacturing industry, variations in machinability are regularly observed when producing the same part out of different material batches of a case hardening steel. Some batches result in variations in chip breakability which leads to a non-robust production process with unforeseen stops of automatic machining process. The aim of the present study is to investigate the influence of the microstructure on chip formation in case hardening steel. Different microstructures were produced from the same batch of material by varying heat treatment. Chips were collected after machining at different feed rates and depths of cut. The cross sections of the chips have been analyzed with respect to overall deformation pattern, mean thickness, and degree of segmentation. Also, the influence of manganese sulfide on machinability has been investigated. The microstructural investigation of the chips has shown that there is a clear difference in the deformation behavior between a case hardening steel with larger and smaller pearlite nodular structure. Chips from the material with larger pearlite nodular size and lower amount of pro-eutectoid ferrite are by far more segmented as compared to chips from materials with smaller pearlite nodular size.

Keywords- Chip Formation; Chip Breakability; Pearlite Nodular Size; MnS Inclusions; Machinability

I. INTRODUCTION

Case hardening steels are commonly used for transmission parts like gear wheels, pinions and crown wheels. The case hardening process produces a carbon-rich surface and provides the part with both enhanced hardness and fatigue life. In general, the part or component undergoes the process of carburizing after it has been machined to final shape. Hence, the product resolves its final microstructure after the machining process. This opens up for the possibility to produce a favorable microstructure for machining by heat treatment without influencing the final strength of the product. However, due to great variety of steels and possible variations resulting from heat treatment conditions, it is important to choose appropriate microstructure for machining process. A microstructure of steel consisting of both ferrite and pearlite in proper proportions shows better machinability as compared to steel consisting of only ferrite or pearlite. The formation of a ferritic and pearlitic microstructure in hypo-eutectoid steels depends primarily on the carbon content and the applied heat treatment process, e.g. isothermal annealing or controlled cooling [1]. However, small deviations in time and temperature during the annealing process can lead to variations in the amount of pro-eutectoid ferrite and pearlite as well as in the pearlite morphology without affecting the overall hardness [1-4]. In manufacturing industry especially gear manufacturing, low carbon steels or low alloy steels are used due to ease of machining. However, variations in machinability are regularly observed when producing the same part out of different material batches of a case hardening steel with an identical chemical composition. For example, some material batches show high tool wear and decreased chip breakability leading to long and/or entangled chips. These types of chips are undesirable since they result in a non-robust production process with unforeseen stops of automatic machining processes. These variations in machinability are due to the broad material specifications in industrial practice such as hardness and strength. Even though case hardening steel falls within this material specification, different microstructures can be obtained with varied phase constituents and phase distributions while keeping the same chemical composition.

Several studies on machining of case hardening steels have been performed with a focus on machinability parameters such as tool wear and cutting parameters [4-7]. Lately, focus has also changed towards new machining techniques such as hard turning. However, little attention has been paid to understand the influence of the microstructure such as pearlite nodular size, phase distribution, pearlite morphology and inclusions on machining. As part of a larger initiative towards a more robust and sustainable gear manufacturing process, it is therefore necessary to study the influence of microstructure on chip breakability in order to obtain better understanding of machining of case hardening steels.

The aim of this study is to acquire better understanding of chip formation when machining case hardening steel of same composition but with different microstructures. In the long run, this knowledge can be used in industry to achieve a more robust machining process. Also, the influence of manganese sulfides on chip formation will be investigated. Simple machining tests are carried out in order to study the chip formation. Even though chips are a by-product of machining operations, they are very important for studying the machining process as they can help in understanding the deformation mechanisms that occur on microscopic level during metal cutting. Hence, in this study, the microstructure of materials and cross sections of chips are analyzed with respect to the effect of non-metallic inclusions, overall deformation pattern, mean thickness and degree of segmentation of the chips.

II. EXPERIMENTAL

A. Materials and Heat Treatment

A typical commercial case hardening steel was used for the present investigation and the chemical composition resembles a 20MnCrS5 according to standard EN10 084 and as presented in Table I.

TABLE I CHEMICAL COMPOSITION (IN WT.%) OF THE INVESTIGATED CASE HARDENING STEEL

C	Si	Mn	P	S	Cr	Mo	Ni	Cu	Sn	Al	Co	N	Nb	V	W
0.205	0.19	1.32	0.018	0.032	1.31	0.08	0.15	0.18	0.011	0.025	0.015	0.011	0.003	0.003	0.002

The steel was continuously cast into billets, hot-rolled to 80 mm diameter cylindrical bars and reduced by turning to a diameter of 50 mm. In order to investigate the influence of microstructure on chip breakability, different heat treatments, i.e. controlled cooling and isothermal annealing were carried out. The same initial material is utilized for the heat treatments. Hence, all materials had the same prior austenitic grain size. Four different microstructures were produced by altering the annealing cycle prior to machining. To obtain wide microstructure variations, three parameters were changed with respect to phase amounts, pearlite nodular size and pearlite morphology, during the annealing treatment: austenitization temperature, holding temperature and holding time for pearlite formation. Large pearlite nodules and high amount of pearlite is obtained in controlled cooling while small nodular pearlite and varied pearlite morphology is achieved when using isothermal annealing. Details about heat treatment, hardness, lamellar spacing and the amount of pro-eutectoid ferrite of these materials are provided in Table II.

TABLE II MATERIAL PROPERTIES

Material	Heat treatment	Hardness (HV ₁₀)	Lamellar distance (μm)	Amount of pro-eutectoid ferrite (%)
LNP	1,200°C-1 h / 630°C-1.5 h (similar to controlled cooling)	186±6	0.27-0.31	15±3
PSP	940°C-1 h/620°C-3 h	164±4	0.23-0.27	47±2
CLP	940°C-1 h/2 min at 250°C/680°C-1 h	163±3	0.26-0.28	41±3
FLP	940°C-1 h/2 min at 250°C/600°C-1 h	180±5	0.19-0.21	43±2

LNP: large nodular pearlite; PSP: partially spheroidized pearlite; CLP: coarse lamellar pearlite; FLP: fine lamellar pearlite.

According to material specification, the hardness values of these different materials are within the specification range (160-200 HV) and their microstructures consist of only pro-eutectoid ferrite and pearlite.

B. Machining

Machining of these materials was performed by longitudinal turning in a Georg Fischer CNC lathe (NDM 17/125). The cutting parameters and the type of insert were selected according to the Volvo Standard Machinability Test used in previous investigations [8, 9]. The cutting data are provided in Table III.

TABLE III CUTTING DATA FOR THE STUDY OF CHIP FORMATION

Tool	Sandvik Coromant; CNMG 120404-PM GC4215
Cutting speed (v_c)	150 m/min
Depth of cut (a_p)	0.5 mm and 2 mm
Feed (f)	Varying (0.05-0.3 mm/r)
Cutting fluid	No

Chips were collected during machining at different feeds and at two different depths. All other cutting parameters were kept constant. Turning was performed on the test bars with same diameter for only few seconds at each feed in order to maintain uniformity. The tools were continuously monitored for not having any type of wear.

C. Characterization

A detailed microstructural study of the heat treated materials and the cross section of the chips was carried out by preparing metallographic samples from the heat treated materials and the chips. The samples for the microstructural investigations were in all cases taken from the outer part of the heat treated bars. The samples were prepared by grinding, polishing, and etching in 3% Nital (HNO₃ and Ethanol) solution. Microstructure characterization of the heat treated materials and the cross section of the chips was performed using a Leica DMRX light optical microscope (OM) and a LEO 1550 Gemini scanning electron microscope (SEM) equipped with EDX analysis. For hardness measurements Vickers hardness method was applied in a Wolpert Dia Tester with 10 kg load (HV10).

III. RESULTS AND DISCUSSION

A. Microstructure of Heat Treated Case Hardening Steels

Figure 1 shows optical micrographs of the four different microstructures taken longitudinal to the rolling direction. Corresponding SEM images of the pearlite lamellar structure are given as insets in Figs. 1b-1d. The four materials are named in this work according to the structure of pearlite as large nodular pearlite (LNP, Fig. 1a), partially spheroidized pearlite (PSP, Fig. 1b), coarse lamellar pearlite (CLP, Fig. 1c) and fine lamellar pearlite (FLP, Fig. 1d).

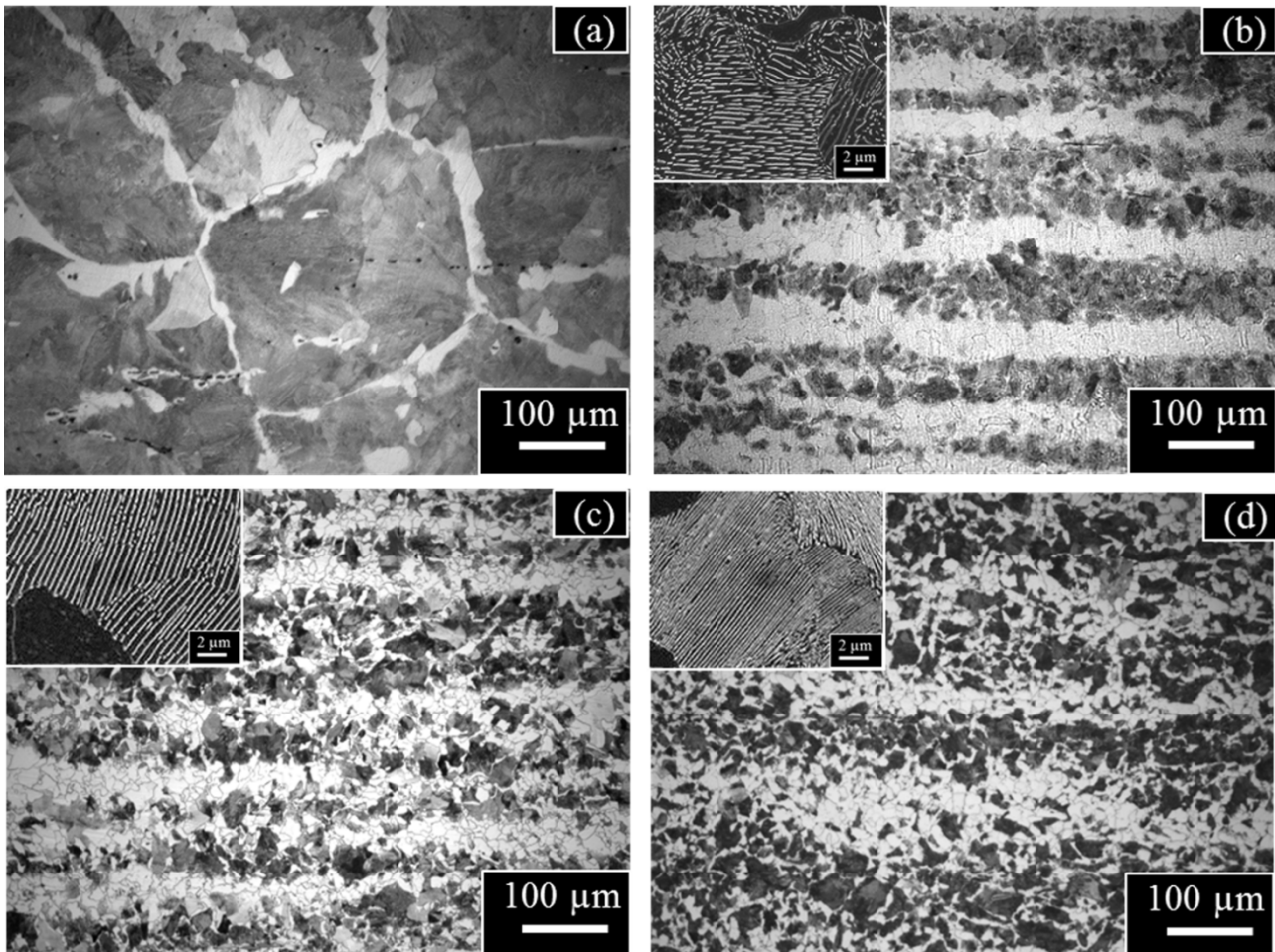


Fig. 1 Optical micrographs of heat treated materials of (a) Large Nodular Pearlite (LNP), (b) Partially Spheroidized Pearlite (PSP), (c) Coarse Lamellar Pearlite (CLP), and (d) Fine Lamellar Pearlite (FLP)

Insets in Fig 1(b)-1(d): Corresponding SEM images of the lamellar structure at higher magnification.

It can be seen in Fig. 1a, the LNP material shows larger pearlite nodules than the other materials and pro-eutectoid ferrite which is distributed along the grain boundaries of the pearlite nodules. The amount of pro-eutectoid ferrite for all four materials is calculated statistically from the optical micrographs and is given in Table II. The amount of pro-eutectoid ferrite in LNP material is with about 15% considerably lower than in the other three materials. Even though the optical micrographs of the materials in Figs. 1b-1d show smaller pearlite nodules, the morphology of pearlite lamellar structure varies between them as shown in the inset SEM images. This difference in pearlite morphologies is due to lower austenitization temperature as well as variations in the holding time and temperature during the subsequent heat treatments (Table II). The different morphologies give also rise to different hardnesses that are provided in Table II. A banded structure can be observed in materials PSP, CLP and FLP (Figs. 1b-1d) and the ferrite band width in these materials varies between 50 and 80 µm. As can be seen in Fig. 1a, there is no banded structure in LNP. Due to the higher amount of pearlite (85%), material LNP shows higher hardness than the other materials. Among the materials with smaller pearlite nodules, material FLP reveals much higher hardness than PSP and CLP even though the amount of pearlite is nearly the same. This is believed to be due to the fine lamellar pearlite in FLP [3, 10].

B. Non-Metallic Inclusions

Figure 2 shows SEM images displaying non-metallic inclusions and its distribution in un-etched samples of material LNP in the rolling direction. Using EDX analysis, the non-metallic inclusions were identified as manganese sulfides (MnS). These

MnS inclusions are elongated and continuous with a large aspect ratio in the rolling direction. Overall, only a few multiphase inclusions were observed and as described before [11]; they consist of aluminum or calcium oxides surrounded by MnS inclusions. The content and distribution of the manganese sulfide inclusions are mainly controlled by the steel making process and their morphology depends on the thermo-mechanical process such as forging or rolling [12]. In the present investigation, the four different materials, LNP, PSP, CLP and FLP are taken from the same batch of material with identical chemical composition. Hence, these samples are assumed to have the same amount and distribution of manganese sulfide inclusions which is also observed in SEM investigations (Fig. 2). After the heat treatments, morphology, shape and amount of manganese sulfide inclusions are not affected and are therefore not measured in detail [13].

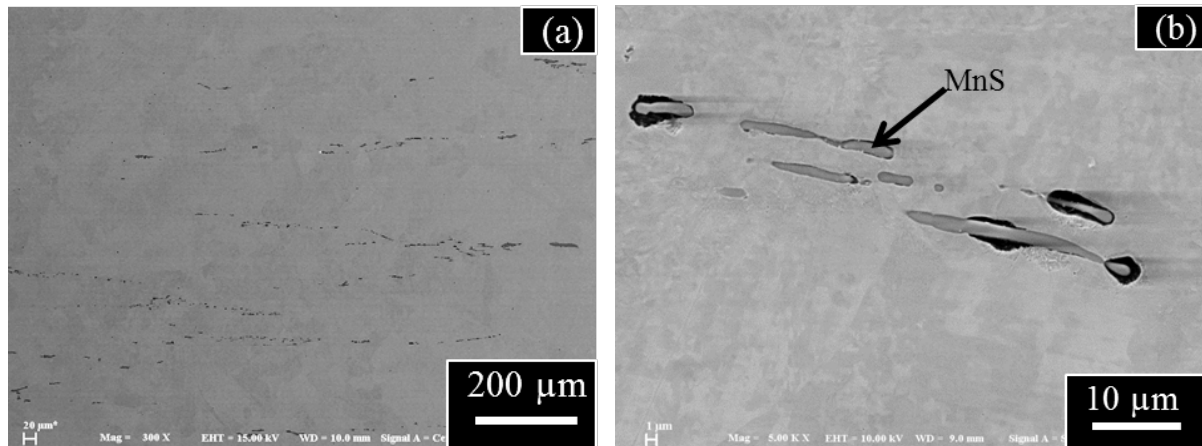


Fig. 2 SEM images of un-etched samples of LNP showing (a) an overview of the MnS distribution and (b) MnS inclusions and voids at higher magnification

The micrographs in Fig. 2b clearly show the presence of voids around the MnS particles as also observed before [14, 15]. The voids are formed as result of the higher coefficient of thermal expansion of MnS, leading to a stronger contraction of the MnS inclusion during cooling as compared to the surrounding steel as well as to compressive circumferential stresses around the MnS inclusions [14]. The MnS inclusions are beneficial for machining as they act as solid lubricant and reduce the coefficient of friction during the machining process [16]. The voids around the MnS inclusions enable the particles to detach easily from the steel matrix during the machining and assist in chip breaking [16].

C. Chip Breakability

The criterion of critical feed [17] was used to study the relationship between chip breakability and material microstructure. The critical feed is the lowest feed without occurrence of chip entanglement or continuous chip formation, i.e. lower critical feed for a material implies good chip breakability. The collected chips after machining were organized in graphs (Fig. 3a and 3b) according to the applied depth of cut in order to compare and study the chip breakability for the four different microstructures (LNP, PSP, CLP and FLP) upon feed.

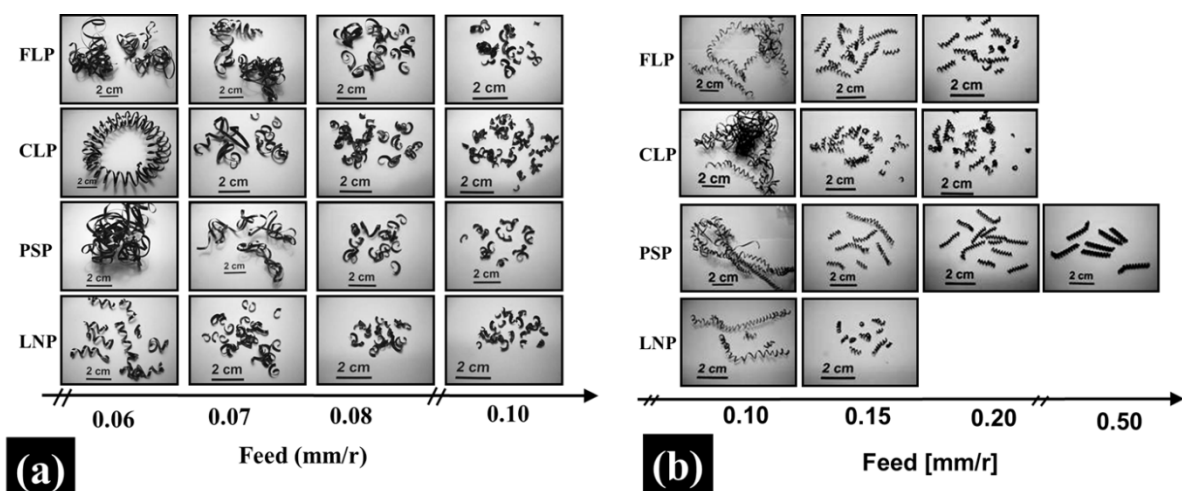


Fig. 3 Comparison of chip breakability for different feeds for the materials LNP, PSP, CLP and FLP at a depth of cut of (a) 2 mm and (b) 0.5 mm

For a depth of cut of 2 mm (Fig. 3a) and feeds equal or above 0.08 mm/r, all materials gave short arc formed chips. Feeds below 0.07 mm/r provided long and entangled chips except for material LNP which still provided short chips down to a feed of 0.04 mm/r. A similar result, i.e. that material LNP behaves different, was obtained when the test was performed with a depth of cut of 0.5 mm. As seen in Fig. 3b, materials PSP, CLP and FLP resulted in continuous entangled chips at a feed of 0.1 mm/r

while material LNP gave shorter non-entangled chips down to a feed of 0.06 mm/r. The results of critical feed for the tested materials are summarized in Fig. 4. Figure 4 reveals that material LNP for both cutting depths displays the lowest critical feed. Hence, the chip breakability test shows that the material with larger pearlite nodular structure (LNP) has a lower critical feed compared to the other materials (PSP, CLP and FLP) and consequently a better chip breakability. For the materials with smaller pearlite nodules (PSP, CLP and FLP), the critical feed is similar, but, as seen from Fig. 3, chip shape can be different. In material CLP and at a cutting depth of 2 mm, the chips are not entangled much, which leads to the slightly lower critical feed. In general, the results reveal that the material with large pearlite nodular structure provides the best chip breakability among these four different microstructures.

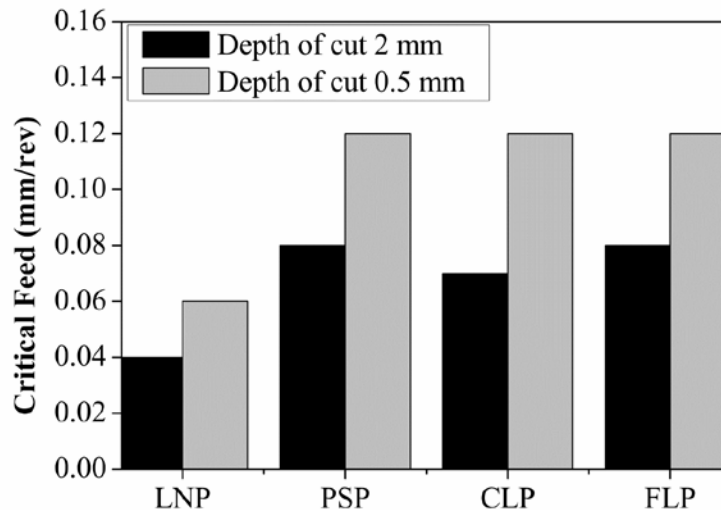


Fig. 4 Critical feed at a cutting depth of 2 mm and 0.5 mm for the tested materials

Figure 5 shows OM images of chips obtained from all four materials obtained with 2 mm depth of cut and a feed of 0.05 mm/rev. Chip thickness and cutting forces are found to be similar for the four materials. However, in LNP, we observed locally thinner chips as well. Also chip segmentation is higher in LNP (Fig. 5a) as compared to the chips of the other three materials (Figs. 5b-5d).

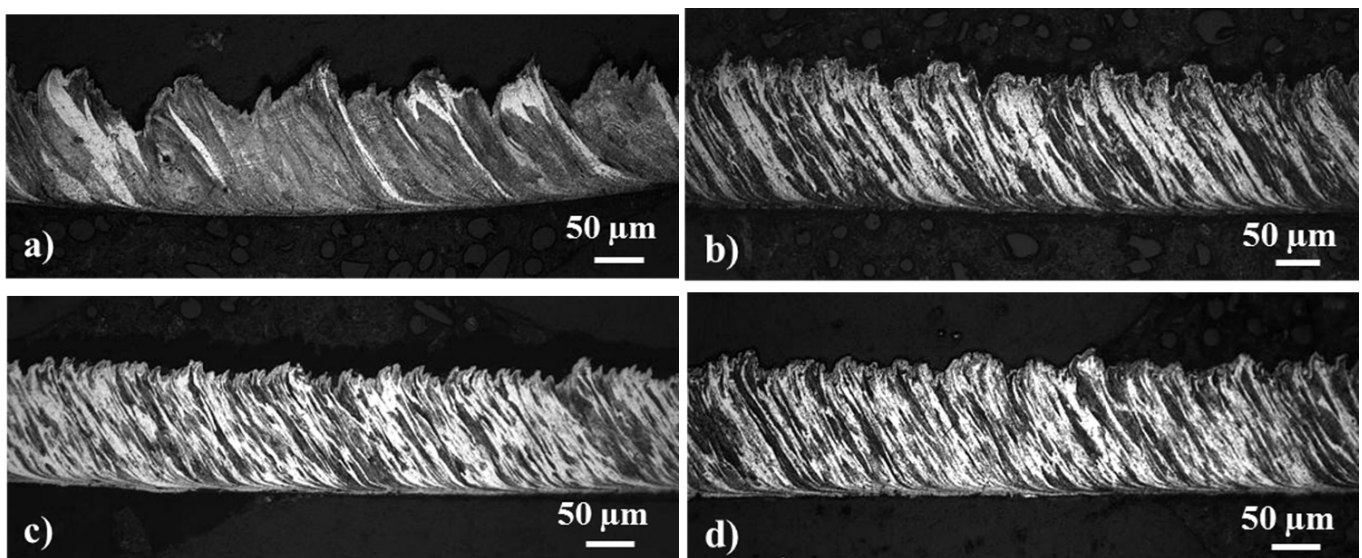


Fig. 5 Comparison of chip morphology in materials LNP, PSP, CLP and FLP

The degree of chip segmentation was measured as the difference between the maximum and minimum thickness of the chip (t_{\max} and t_{\min}). The degree of chip segmentation ($t_{\max} - t_{\min}$) was calculated based on 30 measurements performed on 6 different chips. The measured values of the degree of chip segmentation are given in Fig. 6. Detailed investigations of these chips by SEM revealed that the degree of segmentation is connected to the nodular size of pearlite, in other words the grain size is related to the degree of chip segmentation. As can be seen from Fig. 5a, the distance between the two minimum thickness points in the chip of material LNP is approximately equal to the nodular size of pearlite in the material (compare Fig. 1a).

Similarly, segmentation in the other materials is lower and can be directly related to the nodular size in the corresponding materials.

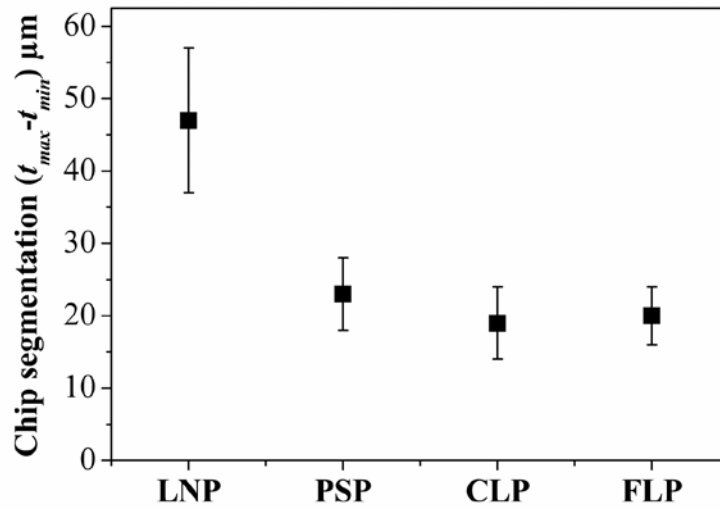


Fig. 6 Degree of chip segmentation of the different materials

D. Microstructure of Chips

In Figures 7a and 7b, chips of material LNP are seen in cross section. The chips were produced at 2 mm depth of cut and a feed of 0.05 mm/rev. As can be seen in Fig. 7a, the MnS inclusion is stretching over the whole cross section of the chip creating a continuous deformed MnS. Figure 7b shows a higher magnification SEM image of the LNP material and the formation of cavities along the MnS inclusions. During machining, the voids around the elongated MnS inclusions reduce the shear stress required for fracture which leads to easy shear or fracture of the chip [18] in the area of minimum chip thickness. Thus, the higher chip breakability observed in LNP is due to the existence of MnS inclusions and the high degree of chip segmentation.

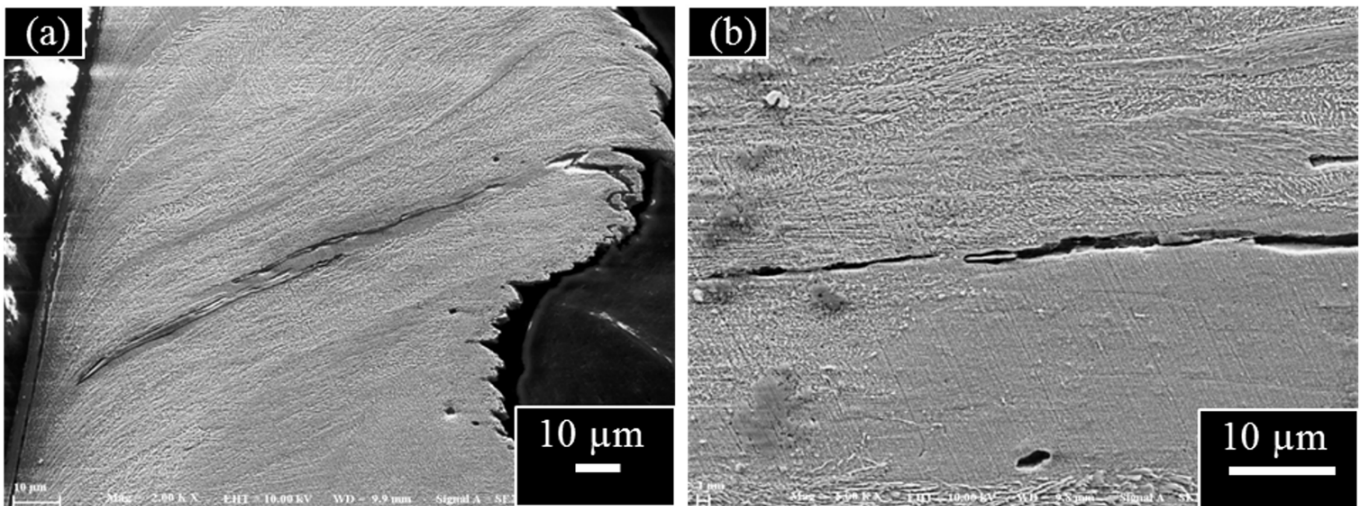


Fig. 7 SEM images of the cross section of chips of material LNP: (a) MnS inclusions reaching over the whole cross section of the chip and (b) High magnification SEM image showing the effect of MnS during machining

In chip cross sections of materials PSP, CLP and FLP, similar types of elongated and deformed MnS inclusions were observed. However, the lower degree of segmentation in these materials as compared to LNP leads to lower chip breakability.

IV. CONCLUSIONS

Different microstructures with varied pearlite nodular size and morphology are produced from the same case hardening steel by varying the heat treatment process. Simple machining experiments are used in order to understand the formation of chips with respect to different microstructures of a case hardening steel. The microstructural investigation of the chips has shown that there is a clear difference in the machining behavior when a case hardening steel is having different microstructures. The investigated microstructures reveal the MnS inclusions are of same amount and morphology. The MnS inclusions are

beneficial for the machining process as they extend through the chip, weaken the chip and lead to chip breaking. Apart from the MnS inclusions, chip segmentation is also found to be important for chip breaking. In the present investigation, chip segmentation mainly depends on the grain size of the material. Chips from a material with a larger pearlite nodular size (and lower amount of pro-eutectoid ferrite) are much more segmented as compared to chips from a case hardening steel with smaller pearlite nodular size. The difference in the degree of segmentation explains the difference in chip breakability (LNP versus FLP, CLP and PSP). Moreover, the study indicates, that pearlite morphology only has minor influence on the chip deformation behavior. When considering chip breakability as the most important criterion for machinability in a turning operation, a case hardening steel with large pearlite nodular structure is to be preferred. However, also an increased tool wear can be expected. Hence, there is a trade-off between the tool wear and chip breakability. Thus, to obtain robust machining with optimum tool wear and chip breakability, it is necessary to perform heat treatments that can lead to grain sizes of about 50 to 100 μm and approximately equal amounts of ferrite and pearlite.

V. ACKNOWLEDGEMENTS

The work is performed within the Area of Advance – Production at Chalmers. Volvo Aero Corporation is acknowledged for providing machining equipment, Componenta Wirsbo AB for supplying the material and for helping with heat treatments, and Scania CV for helping with heat treatments and sample preparation. The authors thank VINNOVA for financial support within the scope of FFI-project Sustainable Gear Manufacturing Realization.

REFERENCES

- [1] N. E. Woldman and R. C. Gibbons, *Machinability and machining of metals*, McGraw-Hill, 1951.
- [2] T. V. Rajan, C. P. Sharma, and Ashok Sharma, *Heat treatment principles and techniques*, PHI Learning Pvt. Ltd., 2012.
- [3] F. C. Campbell, *Elements of metallurgy and engineering alloys*, ASM International, 2008.
- [4] Y. Ozcatalbas and F. Ercan. "The effects of heat treatment on the machinability of mild steels," *Journal of Materials Processing Technology*, vol. 136, pp. 227-238, 2003.
- [5] D. J. Naylor, D. T. Llewellyn, and D. M. Keane. "Control of machinability in medium-carbon steels," *Metals Technology* 3.1 pp. 254-271, 1976.
- [6] J. Barry and G. Byrne. "Cutting tool wear in the machining of hardened steels: Part I: Alumina/TiC cutting tool wear," *Wear* 247.2, pp. 139-151, 2001.
- [7] R. Milovic and J. Wallbank. "The machining of low carbon free cutting steels with high speed steel tools," *Journal of Applied Metalworking* 2.4, pp. 249-257, 1983.
- [8] U. ERIKSSON. "The quantitative assessment of machinability," *International Conference on Processing, Microstructure and Properties of Microalloyed and Other Modern High Strength Low Alloy Steels*, Pittsburgh; Pennsylvania; USA, pp. 9-12, 1992.
- [9] K. Björkeborn, U. Klement and H.-B. Oskarson. "Study of microstructural influences on machinability of case hardening steel," *The International Journal of Advanced Manufacturing Technology*, 49, pp. 5-8, 2010.
- [10] G. Krauss, *Steels: processing, structure, and performance*, ASM International, 2005.
- [11] C. Blais, G. L'Espérance, H. LeHuy, C. Forget, "Development of an integrated method for fully characterizing multiphase inclusions and its application to calcium-treated steels," *Materials characterization*, vol. 38, pp. 25-37, 1997.
- [12] A. Ghosh, *Secondary steelmaking: principles and applications*, CRC Press Llc, 2001.
- [13] L. K. Bigelow and M. C. Flemings, *Sulfide inclusions in steel*, DTIC document, Massachusetts Institute of Technology Cambridge, Department of Metallurgy and Materials Science, 1970.
- [14] D. Brooksbank and K. W. Andrews. "Tessellated stresses associated with some inclusions in steel," *J. Iron Steel Inst.*, vol. 207, pp. 474-483, 1969.
- [15] W. Roberts, B. Lehtinen, and K. E. Easterling. "An in situ SEM study of void development around inclusions in steel during plastic deformation," *Acta Metallurgica*, vol. 24, pp. 745-758, 1976.
- [16] A. K. Roy, S. K. Bhattacharyya, and G. Krauss. "The effect of sulphur and niobium on machinability of micro-alloyed steels," *Key Engineering Materials*, vol. 84, pp. 308-330, 1993.
- [17] L. Zhou, *Machining chip-breaking prediction with grooved inserts in steel turning*, Doctoral Diss. Worcester Polytechnic Institute, 2001.
- [18] H. Yaguchi, "Effect of MnS inclusion size on machinability of low-carbon, leaded, resulfurized free-machining steel," *Journal of Applied Metalworking*, vol. 4, pp. 214-225, 1986.